

Promotion of apoplastic oxidative burst by artificially selected *GhCBSX3A* enhances *Verticillium dahliae* resistance in upland cotton

Yihao Zhang^{1,2,3,4,†}, Yuan Yuan^{1,2,†}, Hongfang Xi², Yaning Zhang¹, Chenxu Gao¹, Meng Ma^{1,2}, Qian Huang², Fuguang Li^{1,2,3} and Zhaoen Yang^{1,2,3,*} 

¹Zhengzhou Research Base, National Key Laboratory of Cotton Bio-breeding and Integrated Utilization, Zhengzhou University, Zhengzhou 450001, China,

²National Key Laboratory of Cotton Bio-breeding and Integrated Utilization, Institute of Cotton Research, Chinese Academy of Agricultural Sciences, Anyang 455000, China,

³Western Agricultural Research Center, Chinese Academy of Agricultural Sciences, Changji 831100, Xinjiang, China, and

⁴State Key Laboratory of Wheat and Maize Crop Science, College of Agronomy, National Wheat Innovation Center and Center for Crop Genome Engineering, Zhengzhou 450001, Henan, China

Received 29 November 2023; revised 21 February 2024; accepted 6 March 2024.

*For correspondence (e-mail yangzhaoen0925@126.com)

[†]These authors contributed equally to this work.

SUMMARY

Verticillium wilt (VW) is a devastating disease affecting various plants, including upland cotton, a crucial fiber crop. Despite its impact, the genetic basis underlying cotton's susceptibility or defense against VW remains unclear. Here, we conducted a genome-wide association study on VW phenotyping in upland cotton and identified a locus on A13 that is significantly associated with VW resistance. We then identified a cystathionine β -synthase domain gene at A13 locus, *GhCBSX3A*, which was induced by *Verticillium dahliae*. Functional analysis, including expression silencing in cotton and overexpression in *Arabidopsis thaliana*, confirmed that *GhCBSX3A* is a causal gene at the A13 locus, enhancing SAR-RBOHs-mediated apoplastic oxidative burst. We found allelic variation on the TATA-box of *GhCBSX3A* promoter attenuated its expression in upland cotton, thereby weakening VW resistance. Interestingly, we discovered that altered artificial selection of *GhCBSX3A_R* (an elite allele for VW) under different VW pressures during domestication and other improved processes allows specific human needs to be met. Our findings underscore the importance of *GhCBSX3A* in response to VW, and we propose a model for defense-associated genes being selected depending on the pathogen's pressure. The identified locus and gene serve as promising targets for VW resistance enhancement in cotton through genetic engineering.

Keywords: upland cotton, *Verticillium dahliae*, reactive oxygen species, artificial selection.

INTRODUCTION

Upland cotton (*Gossypium hirsutum* L.) is the most widely cultivated cotton species, supplying more than 90% of global cotton production (He et al., 2021). However, most commercial cultivars exhibit limited resistance to Verticillium wilt (VW), caused by *Verticillium dahliae*, leading to reductions in fiber quality and yield. In fact, severe outbreaks can cause yield losses reaching 30–80% (Zhang et al., 2019). Given the persistence of *V. dahliae* in soil, long-term production practices showed that breeding resistant cultivars is likely the most effective strategy (Shaban et al., 2018). Advances in functional genomics of cotton have made identification of VW resistance loci and

pathogenesis-related genes critical in disease-resistance cotton breeding (Wang, Wang, et al., 2023).

Verticillium dahliae infects plants through the roots and propagates massively in the vascular system, leading to blockage in the water-conducting xylem tissue. This leads to typical VW symptoms, such as desiccated leaf mesophyll and severe vascular bundle browning (Lai et al., 2022). As the disease progresses, physiological and biochemical changes trigger putative defense responses. These include reinforcement of cell wall structures, the hypersensitive response (HR), the development of broad-spectrum systemic acquired resistance (SAR), and accumulation of reactive oxygen species (ROS) (Shaban

et al., 2018). ROS plays a key role in pathogen–plant interactions; pathogen recognition by the plant rapidly triggers an oxidative burst which acts as a secondary messenger to transduce extracellular signals to the nucleus, an essential step for further defense reactions (Heller & Tudzynski, 2011), including the cotton plant's resistance to *V. dahliae* invasion (Wang et al., 2020).

Despite limited understanding of the cotton-*V. dahliae* pathosystem, progress identifying key loci and genes contributing to verticillium wilt resistance in upland cotton is ongoing. A genome-wide association study (GWAS) of upland cotton VW resistance in a natural-variation population revealed that *GhLecRKs-V.9* is the causal gene for Dt11 locus and is essential for VW resistance (Zhang et al., 2021). Li et al. (2017) performed a GWAS using a panel of 299 *G. hirsutum* accessions and identified a significant VW-related locus on At10; further, knockdown of TIR-NBS-LRR (*GhDSC1*) expression resulted in symptoms of disease susceptibility. Additionally, reverse genetics has uncovered more functional cotton genes involved in VW resistance (Yang et al., 2023). Among these, the thioredoxin *GBNRX1* is crucial for maintaining apoplastic ROS homeostasis in response to *V. dahliae* infection in cotton (Li et al., 2016).

Cystathionine β -synthase (CBS) domain-containing proteins (CDCPs) form a large superfamily of proteins with conserved CBS domains. In *Arabidopsis thaliana* and *G. hirsutum*, 33 and 52 putative CDCP genes have been identified, respectively (Ali et al., 2021; Kushwaha et al., 2009). Among them, CDCPs with just a single CBS pair and no other protein domains were termed *CBSX*. *A. thaliana* has five such *CBSXs* (Kushwaha et al., 2009). The *A. thaliana* *CBSX1* and *CBSX2* directly regulate the TRXs activation in the chloroplast as the redox regulators. *CBSX4* positively regulates salinity, oxidative, and heavy metal tolerance in tobacco plants. *AtCBSX3* regulates ROS production of mitochondrial complex II (succinate dehydrogenase) by activating o-type thioredoxin (Trx-o2), playing a pivotal role in regulating plant development and the redox system (Shin et al., 2020). *TaCBSX3* interacts with glutathione S-transferase 6 (TaGSTU6) in the plasma membrane and cytoplasm, and the knockdown of *TaCBSX3* expression reduces wheat resistance to *Blumeria graminis* f. sp. *tritici* (*Bgt*) (Wang, Guo, et al., 2022). Additionally, in rice, *OscBSX3* serves as a positive regulator in resistance

against *Magnaporthe oryzae*, regulated by both SA and JA-mediated signaling pathways (Mou et al., 2015).

In our study, we conducted a GWAS on VW resistance in *G. hirsutum* accessions, focusing on a locus on A13 significantly associated with VW resistance. Hap. A, an ancestral VW resistance haplotype, was distinct with improved haplotype, further leading to high divergence in this region. *GhCBSX3A*, a gene encoding a CBS domain protein emerged as a potential causal gene underlying the A13 locus. Allelic variation in the *GhCBSX3A* promoter attenuated its expression in *G. hirsutum*, further impairing acquired resistance. Our experimental evidence demonstrated that normal expression of *GhCBSX3A* is essential for the RBOHs-mediated apoplastic oxidative burst and induced SAR response to *V. dahliae* infection in cotton. Moreover, heterologous expression of *GhCBSX3A* in *A. thaliana* contributed to pattern-triggered immunity (PTI)- and SAR-ROS production, increasing resistance to *V. dahliae*. We found that the elite *GhCBSX3A* allele for VW resistance was negatively selected for in the domestication process due to the adverse effect on boll weight (BW), leading to a decreased VW resistance in early improved accessions. However, in the subsequent breeding process, the elite *GhCBSX3A* allele for VW resistance was positively selected, resulting in continuous enhancement of VW resistance. Our findings suggest a correlation between variant VW pressures and artificial selection of elite alleles for VW resistance during the *G. hirsutum* improvement process. Accessions carrying elite *GhCBSX3A* could be valuable resources for enhancing VW resistance in cotton.

RESULTS

High divergence fragment on chromosome A13 significantly associated with cotton VW resistance

In our previous study, the thresholds for GWAS were set to a uniform threshold ($5.03E-6$, $P = 1/n$, where n is the effective number of independent single nucleotide polymorphisms [SNPs]), and we identified a locus on A13 (*AYDI3/AYDP2*) significantly associated with VW resistance of upland cotton, as measured by the disease index (DI) and disease plant percentage (DP) (Zhang, Zhang, Ge, et al., 2023). Based on the allelic genotypes of the leader SNP of *AYDI3/AYDP2*, we divided the GWAS panel into two groups (Hap. 1–2), and haplotypes showed significant

Figure 1. Haplotypes analysis on *AYDI3/AYDP2*.

(a) Manhattan plot for *AYDI3/AYDP2* on chromosome A13 and linkage disequilibrium block around *AYDI3/AYDP2* (A13: 87.47–88.47 Mb).

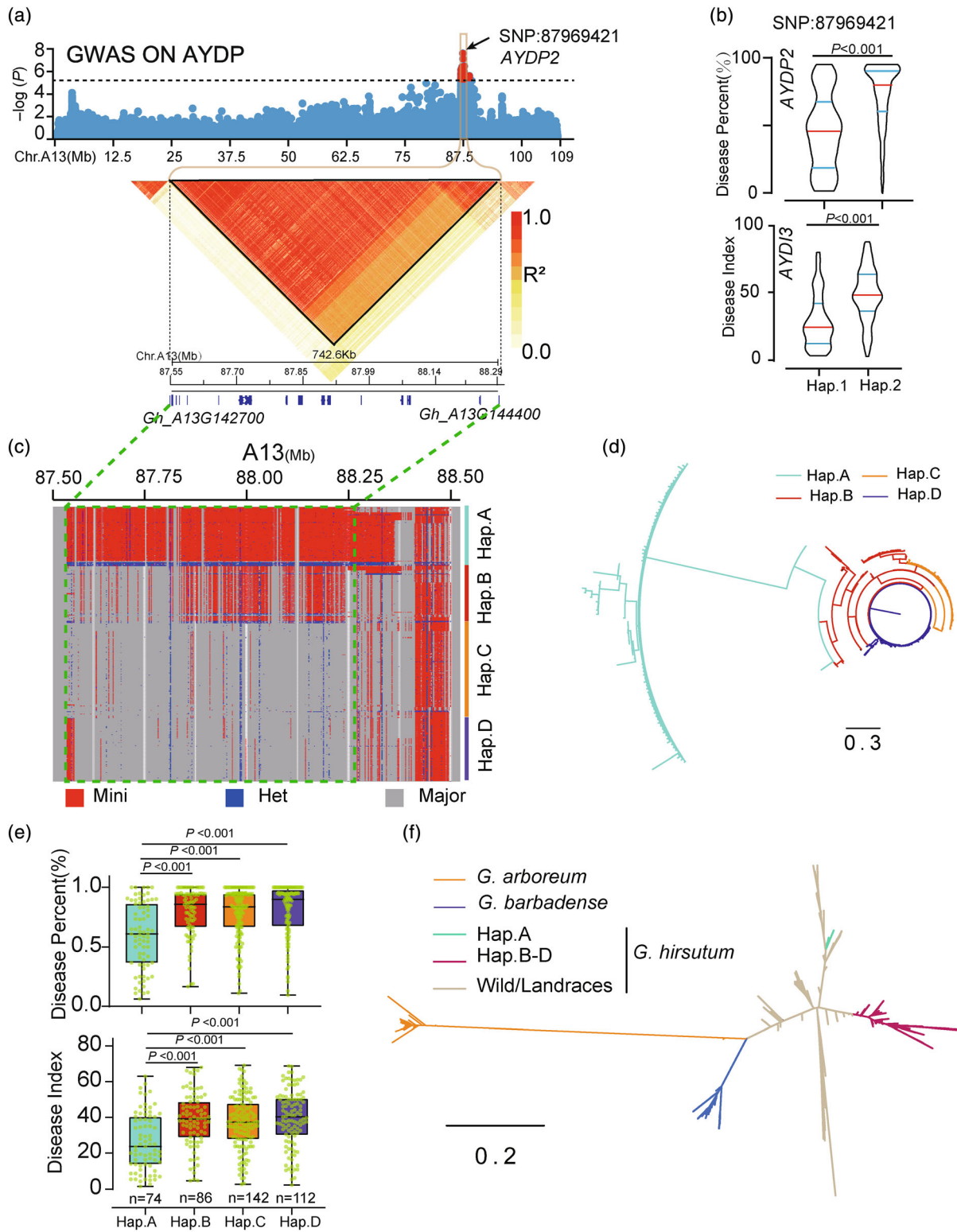
(b) Comparison of DP and DI between the two haplotypes of the leader SNP at *AYDI3/AYDP2* locus.

(c) Haplotypes analysis of *AYDI3/AYDP2*. Five haplotypes (Hap. A–E) were identified. Green box indicates *AYDI3/AYDP2* region.

(d) SNP-based phylogenetic tree harboring 419 accessions of *Gossypium hirsutum* cultivars.

(e) Comparison of DP and DI of the five haplotypes from (c).

(f) SNPs located in *AYDI3/AYDP2* genomic region were used to construct the SNP-based phylogenetic tree comprising *G. hirsutum* cultivars, wild/landrace accessions, *G. barbadense* and *G. arboreum*. All the significances were tested by Student's *t*-test. DI, disease index; DP, disease percentage; SNP, single nucleotide polymorphism.



differences in DI and DP (Figure 1a,b). We then extracted the SNPs located within 1 Mb on either side of leader SNP and calculated the haplotype block, revealing that the genomic spectrum of AYDI3/AYDP2 ranges from 87.55 to

88.29 Mb on A13 (Figure 1a). Interestingly, large amounts of SNP mutations were detected on AYDI3/AYDP2 locus and four distinct haplotypes (Hap. A–D) emerged at this locus in *G. hirsutum* (Figure 1c). Subsequently, a phylogenetic tree

was constructed using the SNPs on *AYDI3/AYDP2*, and it showed that Hap. B–D were clustered together with high similarity, but Hap. A exhibited substantial differences from the other accessions (Figure 1d), underscoring the strong differentiation in this region. Accessions carrying Hap. A showed greater tolerance to *V. dahliae* compared to those carrying Hap. B, C, or D (Figure 1e).

To investigate the donor of Hap. A in *AYDI3/AYDP2*, we constructed an expanded SNP-based phylogenetic tree using the SNPs within *AYDI3/AYDP2* from *G. arboreum*, *G. barbadense*, *G. hirsutum* cultivars, and *G. hirsutum* landraces. The results indicated a distinct separation between *G. arboreum* and *G. barbadense* from *G. hirsutum*, suggesting that the Hap. A are not due to introgression. Interestingly, Hap. A emerged as distinct from Hap. B–D, but it clustered with *G. hirsutum* landraces, indicating that Hap. A could be an ancestral haplotype and contributed to stronger VW resistance (Figure 1f).

Prediction of candidate genes for Verticillium wilt resistance from *AYDI3/AYDP2*

Subsequently, a 742 Kb haplotype block encompassing 17 candidate genes was found in *AYDI3/AYDP2* locus. Swisprot annotation revealed that some of these genes encode ATP-dependent zinc metalloprotease, CBS domain-containing protein, histidinol dehydrogenase, glyceraldehyde-3-phosphate dehydrogenase, UPF0481 protein, 40S ribosomal protein S19-3, metal tolerance protein 10, proton pump-interactor 1, organic cation/carnitine transporter 3, and Myb family transcription factor APL (Table S1). The mRNA-seq data showed that only nine genes exhibited normal expression (FPKM >1) before and after the inoculation with *V. dahliae*.

Considering the important roles of inducible defense signaling pathways in cotton defense against *V. dahliae* (Zhao et al., 2021), we aimed to identify candidate genes within the fragment utilizing mRNA-seq data from cotton roots. We found that *Gh_A13G143300* and 3 other genes (*Gh_A13G144100*, *Gh_A13G144300*, and *Gh_A13G144400*) were induced after *V. dahliae* treatment (Figure 2a). Quantitative PCR further confirmed the expression levels of these genes, and it also identified *Gh_A13G143300* as the uniquely up-regulated gene in this region at multiple time points under *V. dahliae* invasion (Figure 2b).

To verify the potential function of the four inducible genes, we conducted virus-induced gene silencing (VIGS) experiments. TRV::*CLA1* (*chloroplastos alterados 1* gene) was used as a positive control. One week later, a noticeable symptom of leaf whitening is observed in the leaves of positive control (Figure S2). Plants carrying TRV::*Gh_A13G143300* in three independent silenced lines displayed typical symptoms of VW, showing an 80% percent increase in DI compared with the control (Figure 2c,d). Stem cross sections showed severe browning of vascular

bundles in TRV::*Gh_A13G143300* as well as greater amounts of *V. dahliae* colonization (Figure 2e,f). qPCR results showed a significant reduction in the expression of *Gh_A13G143300* across different lines compared with the control (Figure 2g). Collectively, these experiments identified *Gh_A13G143300* as the major functional gene in *AYDI3/AYDP2*, crucial for the integrity of VW resistance in cotton. *Gh_A13G143300* encodes a single pair of CBS domain (PFAM: 00571) (Figure S1a), and showed a high similarity with *Gh_D13G144500.1* (another copy located on chromosomes D13), *AtCBSX3* (*AT5G10860.1*) and *TaCBSX3* (*XM_020317884.1*). Consequently, we will refer to *Gh_A13G143300* as *CBSX3A* in *G. hirsutum* (*GhCBSX3A*) (Figure S1b).

Allelic variation in the promoter of *GhCBSX3A* attenuated the expression in *G. hirsutum*

We analyzed the *GhCBSX3A* genomic region, including a 3 Kb upstream sequence from the ATG start codon, and identified three polymorphic sites in the potential promoter region and one polymorphic site in intron 3. These polymorphisms were found to have high linkage disequilibrium values between each other ($R^2 > 0.9$) (Figure 3a). We initially cloned the coding sequence of *GhCBSX3A* from both Hap. A (L068, B061, and L101) and Hap. B (L109, L076, and L105), and no polymorphism was identified. Given the importance of normal expression of *GhCBSX3A* for the maintaining of VW resistance in cotton, we investigated the expression of *GhCBSX3A* across different haplotype groups. The results revealed that *GhCBSX3A* expression in Hap. A was significantly higher than in Hap. B–D, both before and after *V. dahliae* inoculation (Figure 3b). These findings were corroborated by quantitative reverse transcriptase PCR (qRT-PCR) experiments, showing that in Hap. A, *GhCBSX3A* expression increased 1.9- and 2.1-fold, respectively, before and after *V. dahliae* inoculation, compared to Hap. B–D (Figure 3c).

Given the observed expression pattern variations of *GhCBSX3A*, we proceeded to validate polymorphisms in potential promoter region (Wu et al., 2022). We cloned 3 Kb upstream sequences of the ATG start codon from Hap. A and Hap. B, respectively. These sequences, displaying high divergence with seven SNPs, were named as *GhCBSX3A_R_{pro}* (resistant) and *GhCBSX3A_S_{pro}* (susceptible), respectively (Figure 3a).

To assess the functional implications of *GhCBSX3A_R_{pro}* and *GhCBSX3A_S_{pro}* in gene expression, we cloned the sequences to drive a firefly *LUC* reporter gene in tobacco cells. We truncated *GhCBSX3A_R_{pro}* to *GhCBSX3A_R_{pro}-1* (3.0 Kb upstream from ATG to 1.6 Kb upstream from ATG) and *GhCBSX3A_R_{pro}-2* (1.6-Kb upstream from ATG). Similarly, we created the promoter fragments *GhCBSX3A_S_{pro}-1* and *GhCBSX3A_S_{pro}-2* in the same pattern (Figure 3d). The results indicated that luciferase (LUC) activity within the

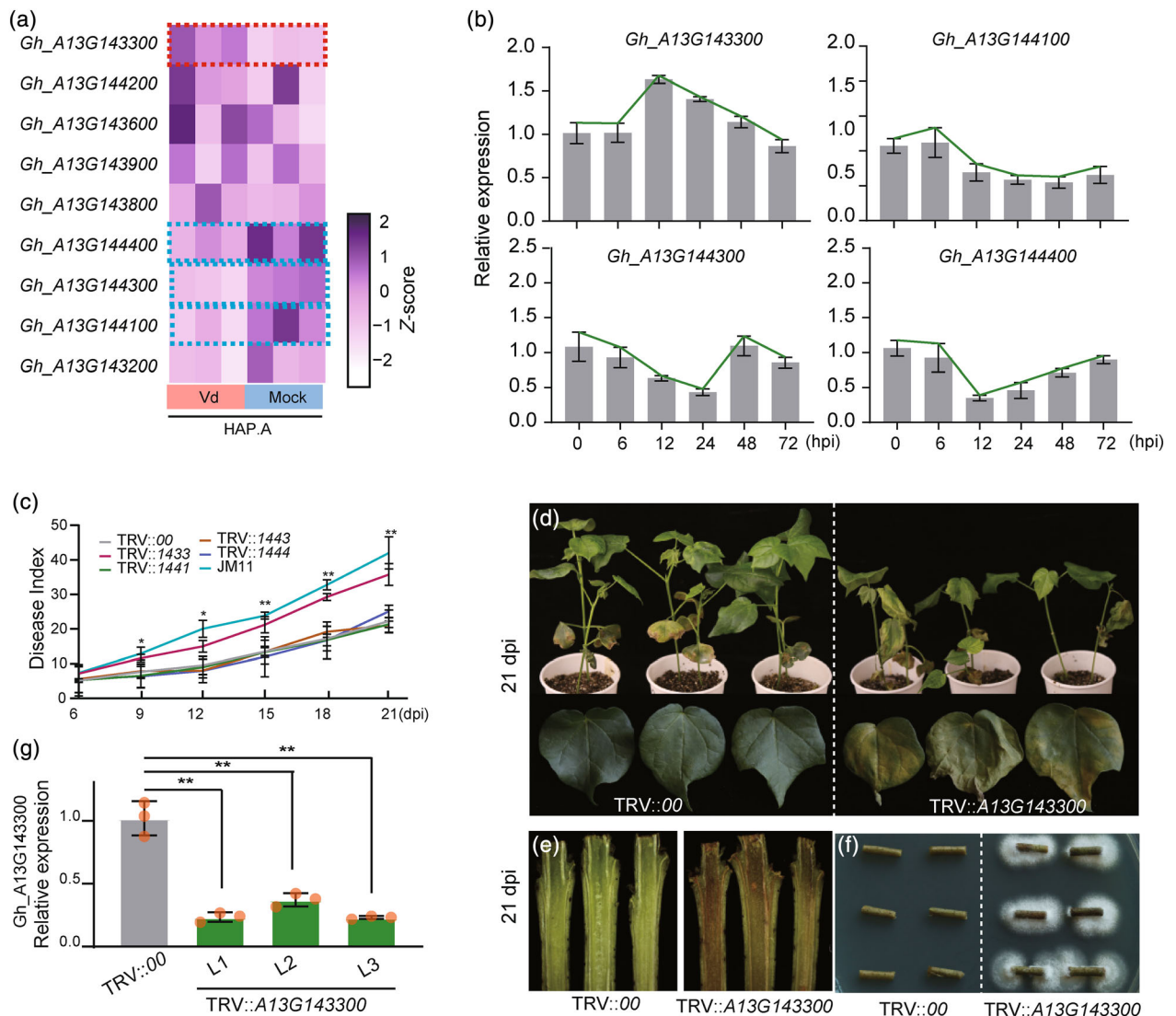


Figure 2. Identification of candidate genes associated with *Verticillium* wilt resistance on *AYDI3/AYDP2*.

(a) Expression level analysis of genes from *AYDI3/AYDP2* based on transcriptome at 24 h post-inoculation with *Verticillium dahliae*. Three replicates are represented. The four genes in the dot line boxes were the candidate genes.

(b) Expression patterns of four candidate genes at 0, 6, 12, 24, 48, and 72 hpi with Vd080 treatment.

(c) Disease indices were measured at 6, 9, 12, 15, 18 and 21 dpi. JM11 was used as susceptible control. TRV::00 was used as a negative control.

(d–f) Plant wilt phenotype, stem browning symptoms, and fungal recovery experiments of TRV::00 and TRV:: *Gh_A13G143200* were photographed at 21 days post-inoculation.

(g) Expression levels of target genes in three virus-induced gene silencing lines. *P*-values obtained from Student's *t*-test, * and ** indicates $P < 0.05$ and $P < 0.01$ respectively.

region transformed with *GhCBSX3A_{R_{pro}-1}::LUC* was comparable to *GhCBSX3A_{S_{pro}-1}::LUC*. However, *GhCBSX3A_{R_{pro}-2}::LUC* consistently exhibited higher reporter activity in tobacco cells than the *GhCBSX3A_{S_{pro}-2}::LUC* did (Figure 3e). Further evaluation of LUC activity confirmed these findings, suggesting that the difference in *GhCBSX3A* expression levels depend on the mutations between *GhCBSX3A_{R_{pro}-2}* and *GhCBSX3A_{S_{pro}-2}*.

Building on this idea, we constructed a series of truncated *GhCBSX3A_{S_{pro}-2}* and *GhCBSX3A_{R_{pro}-2}* derivatives.

These were used to drive a firefly *LUC* reporter gene with the help of a 35Smini promoter. We observed significant differences in LUC activity between promoters with and without the mutations (T/C) on the third nucleotides bases of canonical TATA-box sequence 5'-TATAAA-3' (Patikoglou et al., 1999; Zhao et al., 2018) (Figure 3f). To further investigate the function variation of TATA-box between *GhCBSX3A_{S_{pro}}* and *GhCBSX3A_{R_{pro}}* we constructed three tandem copies of the TATA-box sequence to similarly drive a firefly *LUC* reporter gene with the help of 35Smini promoter (Figure 3g). As

6 Yihao Zhang et al.

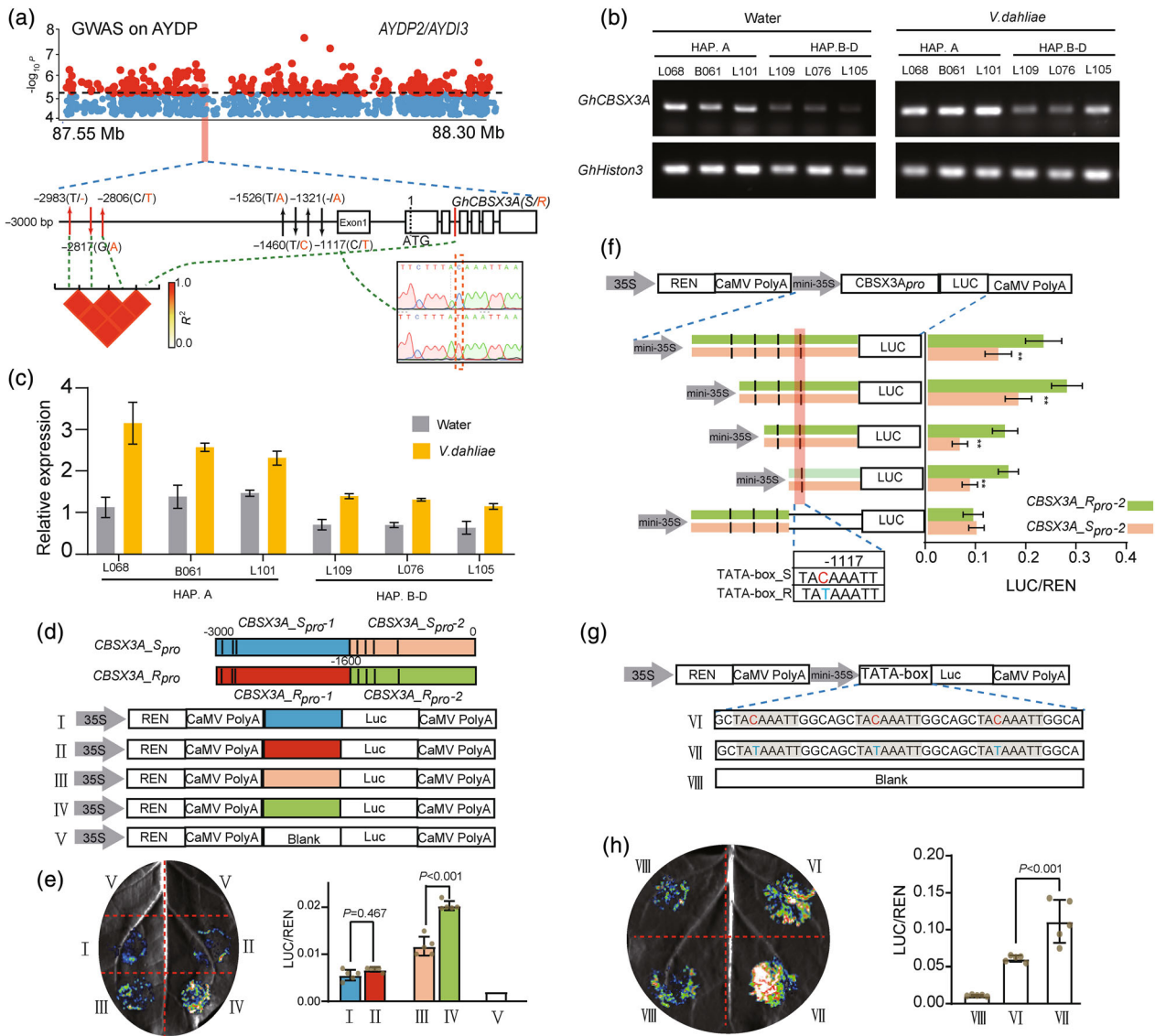


Figure 3. Highly divergent of *GhCBSX3A* promoter mediates different transcriptional activity. (a) An illustration of seven SNPs in the *GhCBSX3A* promoter. *GhCBSX3A_S* and *GhCBSX3A_R* are represented by black and orange text, respectively. (b) Expression level analysis of *GhCBSX3A* using semi-quantitative PCR; *GhHistone3* was used as an internal control. (c) Expression level analysis of *GhCBSX3A* in Hap. A–D using qRT-PCR. Expression levels were measured at 24 hpi using the root. (d) Diagrams of the luciferase reporter constructs used for transient expression analysis. The promoter of each allele was split into two segments marked by blue and orange or red and green color. The four segments were integrated into REN/LUC vectors named as I to IV, empty vector was used as control and named as V. (e) Transcriptional activities of the recombinant vectors in (d) were determined by transient expression of a luciferase reporter in tobacco leaves. The value of LUC was normalized to that of REN, All presented *P* values correspond to two-sided *P* values using Student's *t*-test. (f) Diagrams of the luciferase reporter constructs, in which truncated sequences of *GhCBSX3A_R/Spro-2* were constructed upstream of LUC reporter, REN/LUC was calculated. Significant difference was measured between different groups (Student's *t* test), * and ** indicate *P* < 0.05 and *P* < 0.01, respectively. The marked substitution at positions –1117 resulted in difference in LUC activity between *GhCBSX3A_Rpro-2* and *GhCBSX3A_Spro-2*. (g) The 3 × TATA-box core sequence from *GhCBSX3A_Spro-2* and *GhCBSX3A_Rpro-2* were utilized to drive a firefly LUC reporter gene with the help of 35Smini promoter and named as VI and VII, respectively. Empty vector was used as control and named as VIII. (h) Activities of the vectors in (g) were measured in tobacco leaf. All the significances were tested by the Student's *t*-test. SNP, single nucleotide polymorphism.

expected, TATA_R::LUC showed consistently higher reporter activity in tobacco cells compared to the TATA_S::LUC (Figure 3h). Collectively, these results indicated that allelic variation on TATA-box of *GhCBSX3A* promoter attenuated its expression in *G. hirsutum*.

Apoplastic oxidative burst after inoculation with *V. dahliae* depends on normal expression of *GhCBSX3A*

In previous studies, knockdown of *AtCBSX3* revealed anther indehiscence due to deficient lignin deposition

caused by insufficient ROS accumulation (Shin et al., 2020). Considering ROS are key players in pathogen–plant interactions (Heller & Tudzynski, 2011), we conducted a comparative analysis of ROS during the early stages of *V. dahliae* invasion in *GhCBSX3A* silencing lines. Our results revealed that *V. dahliae* infection induced H_2O_2 production in control leaves, but the knockdown of *GhCBSX3A* expression inhibited the accumulation of H_2O_2 both under normal condition and *V. dahliae* infection (Figure 4a). Subsequently, we determined H_2O_2 concentrations in roots with a UV-spectrophotometer. H_2O_2 concentrations in the control were significantly induced following *V. dahliae* invasion and had peak values at 3 and 15 h post-inoculation (hpi). Remarkably, silencing *GhCBSX3A* not only delayed the two peaks of H_2O_2 induction but also significantly decreased H_2O_2 accumulation during the *V. dahliae* infection (Figure 4b).

To understand why H_2O_2 induction was inhibited in *GhCBSX3A* silenced lines, we evaluated the expression of major enzymes involved in ROS signaling. Previous studies have indicated that the rapid and transient production of ROS by plants is mainly caused by membrane-associated respiratory burst oxidase homologs (RBOHs) (Li, Zhao, et al., 2021). Our results showed *GhRBOHBs* and *GhRBOHDs* were significantly up-regulated in TRV::00 after *V. dahliae* inoculation (Figure 4c) which aligns with findings in *G. barbadense*, where homologous genes were identified as major functional RBOHs in cotton against biotic stress (Chang et al., 2020). Remarkably, when *GhCBSX3A* expression was transiently suppressed, the induction of *GhRBOHBs* and *GhRBOHDs*

following *V. dahliae* inoculation was reduced or absent. Additionally, we analyzed the expression of catalase (CAT) and scorbate peroxidase (APX), considered to be major genes encoding ROS-scavenging enzymes (Zhu et al., 2020). qRT-PCR results suggest that expression of ROS-scavenging enzymes was not significantly induced in the early stage of *V. dahliae* invasion in either group, and the knockdown of *GhCBSX3A* did not affect the ROS scavenging process (Figure 4c). *WRKY40* and *GSTF8* were identified as important downstream genes in response to ROS (Shin et al., 2020), and further investigation revealed that *WRKY40* was significantly induced in both TRV::00 and TRV:: *GhCBSX3A*, with the induction being significantly greater in the former.

Previous studies have linked plant resistance to pathogens, mediated by ROS accumulation, with SAR and HR (Liu & Zhang, 2021; Vlot et al., 2021). HRs are characterized by several active physiological responses that restrict pathogen colonization and stimulate the expression of HR markers, such as *HIN1* and *HSR203J* (Zhang et al., 2016). These markers were significantly up-regulated in both TRV::00 and TRV:: *GhCBSX3A* lines, and the knockdown of *GhCBSX3A* had no effect on HR response following *V. dahliae* infection. SAR, a type of long-distance immunity in plants, provides long-lasting resistance to a broad spectrum of pathogens (Gruner et al., 2018), and it is marked by *NPR1* and *PR1* (Zhang et al., 2016). In our study, the expression of *PR1* was induced only in the control group, and it was significantly decreased in TRV:: *GhCBSX3A* lines compared to TRV::00 both before and after inoculation (Figure 4d).

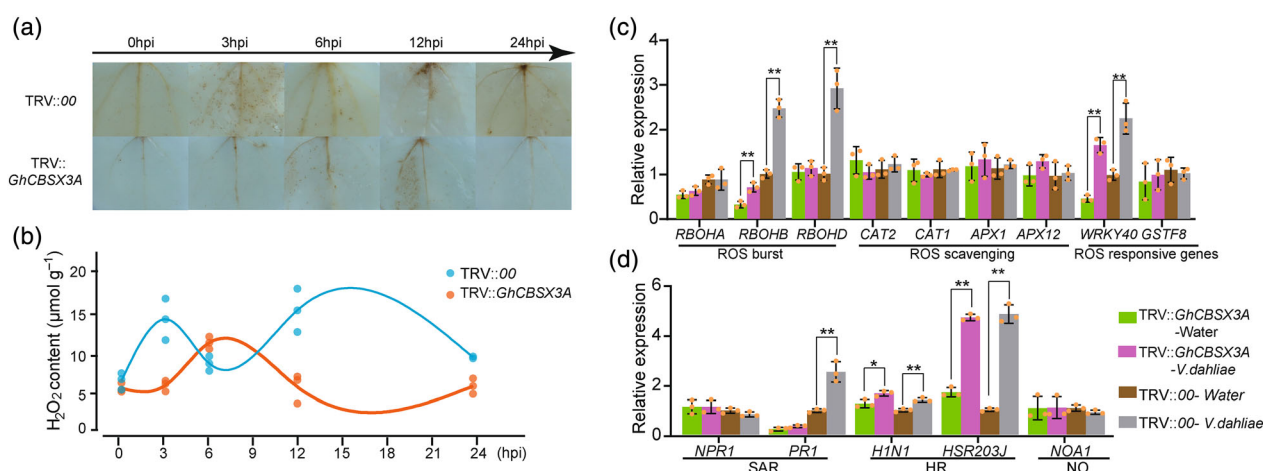


Figure 4. *GhCBSX3A* silencing cotton attenuates the apoplastic oxidative burst. (a) 3, 3'-Diaminobenzidine staining to indicate H_2O_2 accumulation in TRV:: *GhCBSX3A* at 0, 3, 6, 12, and 24 h post-inoculation with *Verticillium dahliae*. TRV::00 was used as negative control. (b) H_2O_2 concentrations in roots were determined by UV spectrophotometer method. (c) Relative expression of major enzymes involved in reactive oxygen species signaling. Leaves of TRV::00 and TRV:: *GhCBSX3A* plant were collected for RNA extraction at 12 hpi. Significant difference was measured between different groups (Student's *t* test), * and ** indicate $P < 0.05$ and $P < 0.01$, respectively. (d) Relative expression of marker genes of systemic acquired resistance (SAR) and hypersensitive response (HR) at 12 hpi.

In addition to ROS, reactive nitrogen species, comprising nitric oxide (NO) can also serve as key regulatory signals during pathogen infection. Nitric oxide associated 1 (NOA1) protein is implicated in plant disease resistance and NO biosynthesis (Qi et al., 2018). The expression of *NOA1* was not induced by *V. dahliae* infection in both TRV::00 and TRV::*GhCBSX3A* lines (Figure 4d). Taken together, these results indicated that the knockdown of *GhCBSX3A* expression compromised the integrity of SAR, and further reduced RBOHs-mediated apoplastic oxidative burst and VW resistance in cotton.

Heterologous expression of *GhCBSX3A* in *Arabidopsis* leads to enhanced resistance to *V. dahliae* via contribution to PTI- and SAR-ROS production

To generate overexpression lines, we expressed *GhCBSX3A* in *A. thaliana* under the control of a CaMV 35S promoter. Interestingly, we observed that 35S::*GhCBSX3A* significantly decreased the germination rate (Figure S4a). After growing seedlings under normal condition for 3 weeks, the root length of OE-3 and OE-7 were reduced by 28 and 49% compared to the WT, respectively (Figure 5a–c).

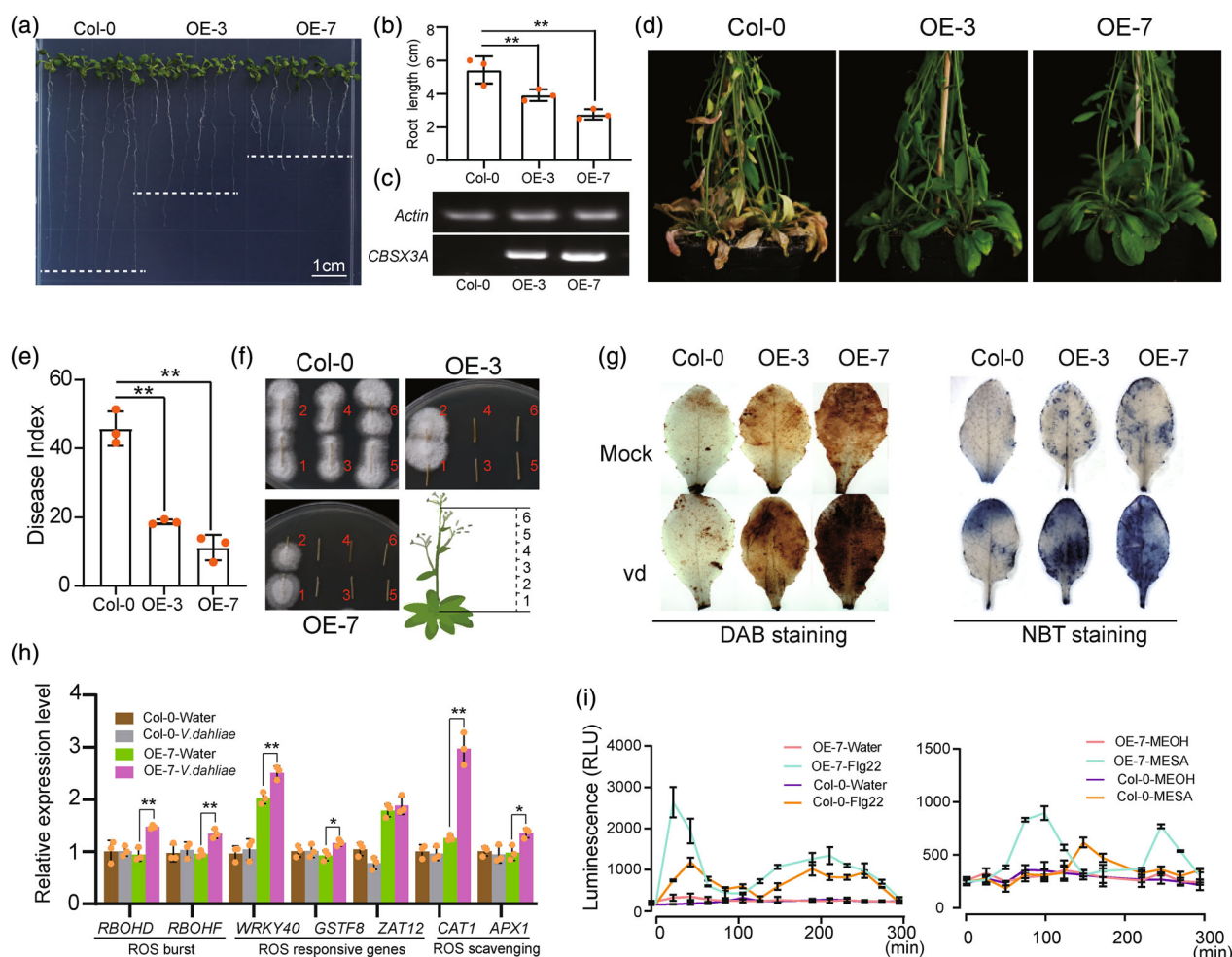


Figure 5. Overexpression of *GhCBSX3A* enhanced *Verticillium* wilt tolerance in *Arabidopsis thaliana*.

(a, b) Phenotyping of 3-week-old OE seedlings (a), and the root length comparison among OE lines and Col-0 (WT) (b). The bar represented the standard deviation of three independent experiments, * and ** indicate $P < 0.05$ and $P < 0.01$, respectively. (c) Expression level detection of *GhCBSX3A* using semi-quantitative PCR. *A. thaliana Actin* was used as an internal control. (d–f) *A. thaliana* seedlings were inoculated with *Verticillium dahliae*. Plant wilt phenotype of OE lines and Col-0 were photographed at 3 weeks post-inoculation (d), and disease index was measured at same time point (e). Sections of inoculated seedlings were used for fungal recovery experiments and photographed after 7 days (f). The positions of each section corresponded to diagrammatic drawing. (g) 3, 3'-Diaminobenzidine (DAB) staining for H_2O_2 and nitroblue tetrazolium (NBT) staining for O_2^- in *A. thaliana* leaves at 24 h post-inoculation with *V. dahliae*. (h) Relative expression of major enzymes involved in ROS signaling, leaves of OE-7 and Col-0 were collected for RNA extraction at 12 hpi. (i) ROS production in Col-0 and OE-7 upon treatment with Flg22 and MeSA, with leaves treated with water and MEOH serving as negative control, respectively. ROS, reactive oxygen species.

However, the aboveground tissue growth patterns were very similar, akin to the function of *AtCBSX3* in negative regulation of plant growth (Shin et al., 2020). Subsequently, 35S::*GhCBSX3A* and Col-0 plants were infected with Vd080 strain to evaluate the gene function of *V. dahliae* resistance. The results showed enhanced resistance in both overexpression lines in *A. thaliana* compared with control, with the DI in OE-3 and OE-7 decreased by 59 and 75%, respectively, compared to the WT (Figure 5d,e). We next isolated *V. dahliae* from different stem nodes of Col-0 and the overexpression lines. The Col-0 plants exhibited a high load of culturable *V. dahliae* in explants across all stem nodes of different heights, whereas *V. dahliae* was only isolated from the first and second stem nodes in the overexpression lines (Figure 5f). This suggests that *GhCBSX3A* expression confers a higher resistance to *V. dahliae* colonization, further inhibiting disease progression throughout the whole invasion period.

Considering the role of *GhCBSX3A* in ROS-mediated *V. dahliae* resistance in cotton, we compared various ROS components between Col-0 and overexpression lines. Prior to and post-*V. dahliae* infection, we detected increased accumulation of H₂O₂ and O₂⁻ in OE-3 and OE-7 compared to Col-0 (Figure 5g). Furthermore, we assessed the expression of major enzymes involved in ROS signaling in *A. thaliana*. *RBOHD* and *RBOHF*, which are pleiotropic and mediate diverse physiological processes including the response to pathogens (Morales et al., 2016), were significantly induced only in 35S::*GhCBSX3A* during early *V. dahliae* infection. Further investigation revealed that the expression of ROS-regulated genes (*WRKY40*, *GSTF8*, and *ZAT12*) (Lunn et al., 2022; Shin et al., 2020) was significantly higher in 35S::*GhCBSX3A* lines than in Col-0 (Figure 5h). Contrasting with the negligible effects on the expression of ROS scavenging genes in Col-0 under *V. dahliae* treatment, overexpression of *GhCBSX3A* enhanced the induction of *CAT1* and *APX1* after *V. dahliae* infection, and it increased the expression of *ZAT12* both before and after inoculation (Figure 5h). These findings indicate that heterologous expression of *GhCBSX3A* mediated an intense response to oxidative stress under both normal condition and during *V. dahliae* invasion.

RBOHs mediate the production of ROS during pathogen infection primarily depends on pathogen-associated molecular PTI and SAR, which is activated in response to various immune elicitors (Li, Zhao, et al., 2021). To examine the possibility of the specific role of *GhCBSX3A* in PTI-mediated ROS production, we compared the production of ROS in Col-0 and OE-7 following treatment with Flg22, a well-charactered PTI elicitors (Li, Zhao, et al., 2021). Our results showed that OE-7 exhibited an earlier and higher peak of ROS production compared to the Col-0 after Flg22 treatment (Figure 5i). Moreover, we assessed SAR-ROS production by treating Col-0 and OE-7

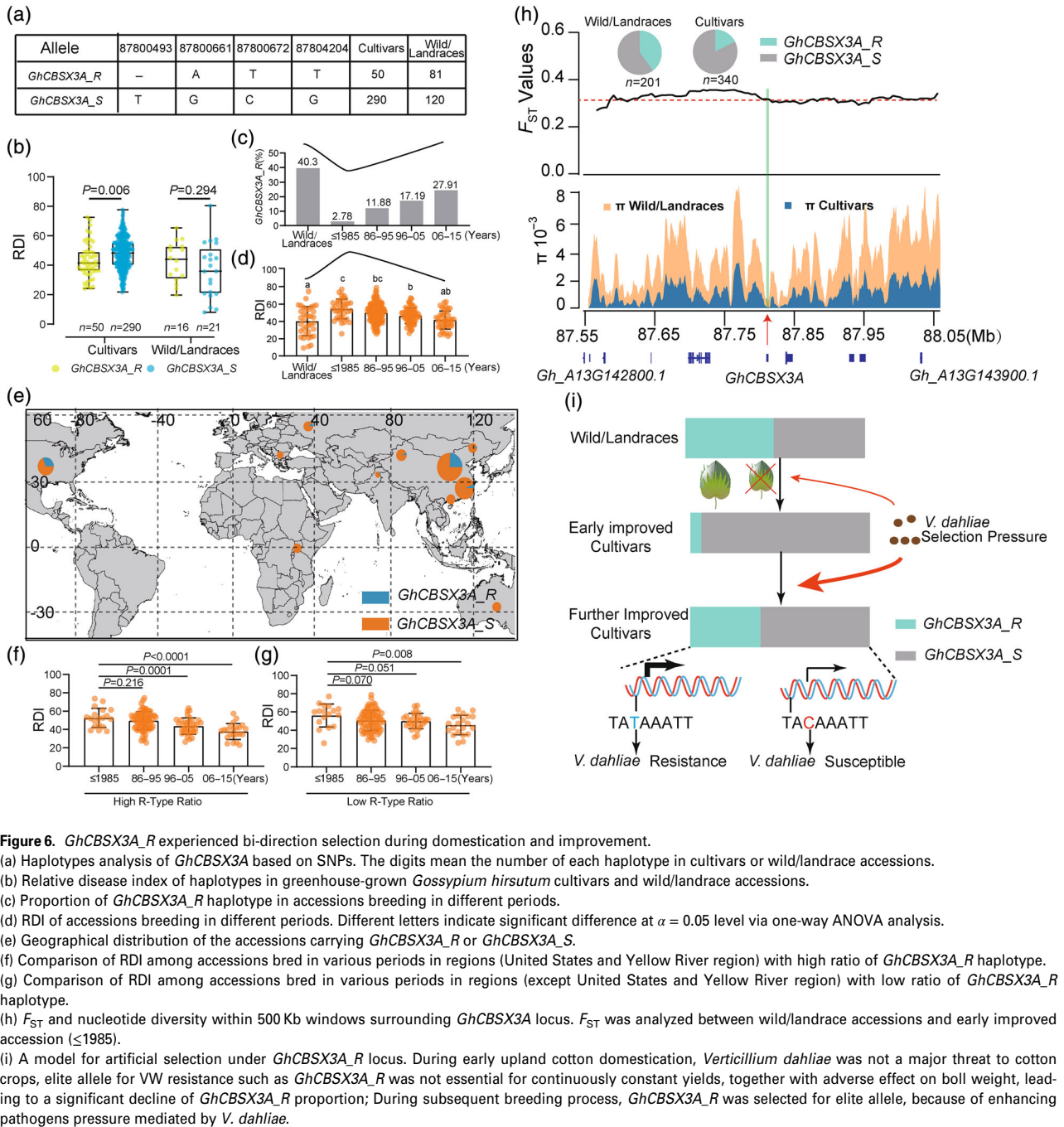
with methyl salicylic acid (MeSA) and found that OE-7 showed significantly increased ROS production compared to the Col-0 (Figure 5i). Viewed together, these results suggest that in *A. thaliana*, *GhCBSX3A* positively regulates a broad-spectrum of RBOHs-mediated ROS signaling, including both PTI and SAR. This leads to subsequent immune responses and enhanced *V. dahliae* resistance.

***GhCBSX3A_R* haplotype experienced bi-direction selection during domestication and improvement**

To analyze the effects of domestication on *GhCBSX3A* locus, we focused on the VW DI of 340 cultivars and 37 wild/landrace accessions harboring either the *GhCBSX3A_R* or *GhCBSX3A_S* allele (Zhang, Zhang, Gao, et al., 2023). Our analysis showed that the *GhCBSX3A_R* allele was more common in wild/landrace accessions (81 of 201 accessions), but it was less frequent in improved upland cotton (50 of 370 accessions) (Figure 6a). Interestingly, there was no discernible variation in VW resistance between the accessions carrying *GhCBSX3A_R* and those carrying *GhCBSX3A_S* in wild/landrace accessions, but those cultivars carrying *GhCBSX3A_R* exhibited greater tolerance to VW than those carrying *GhCBSX3A_S* (Figure 6b). These findings suggest that the elite allele *GhCBSX3A_R*, which confers VW resistance in cultivars, has originated in wild cotton prior to domestication.

To further investigate the artificial selection process of *GhCBSX3A_R*, we evaluated the proportion of *GhCBSX3A_R* in accessions bred during different periods (Figure 6c; Table S2). We found that wild/landrace accessions exhibited the highest frequency of *GhCBSX3A_R*. However, this elite allele for VW resistance was quite rare in the early improved accessions before year 1985 (2.78%). Notably, the proportion of *GhCBSX3A_R* increased significantly in cultivated *G. hirsutum* during subsequent breeding improvements, rising more than 10-fold after year 2006 compared to early improved accessions (Figure 6c). We also evaluated the VW resistance of accessions bred in various periods. Wild/landrace accessions exhibited the highest VW resistance, whereas the early improved lines were the most susceptible to *V. dahliae*. Similar to the increased proportion of *GhCBSX3A_R*, VW resistance improved continuously during subsequent breeding process (Figure 6d). These results indicate that genetic improvement from wild/landrace accessions to improved upland cotton was accompanied by a significant reduction in VW resistance and a loss of the *GhCBSX3A_R* allele. Nevertheless, during subsequent breeding process, increasing proportion of *GhCBSX3A_R* was observed alongside continuous improvements in VW resistance. Yet, as of now, neither VW resistance nor the proportion of dominant alleles has returned to the levels observed in wild/landrace accessions.

Natural plant populations often experience strong pathogen pressure and defense-associated genes are known to be under selection dependent on these



pressures. A variable distribution results in subpopulations that encounter different environmental challenges (Kahlon et al., 2020). Although *GhCBSX3A_R* allele in cultivars is distributed worldwide, it is more prevalent in the United States and the Yellow River region of China, with frequencies of 27.9 and 20.2%, respectively (Figure 6e). Historically, *V. dahliae* was introduced to most of China's cotton planting areas from the United States in the 1930s through seed transmission, and the most destructive outbreaks of

VW occurred in the Yellow River region in 1990s, where disease incidence surpassed 90% (Tan, 1994; Wang, 2015). This pattern suggests a potential relationship between regional VW-mediated challenges and variation in the *GhCBSX3A* allele. To further investigate the artificial selection associated with VW resistance at the *GhCBSX3A* locus, we compared the VW resistance evolution in regions with high and low proportions of the *GhCBSX3A_R* allele. Our findings revealed continuous improvement in VW

resistance in two groups, with significantly greater progress in areas with a higher frequency of *GhCBSX3A_R* (Figure 6f,g). This supports the notion that the *GhCBSX3A_R* allele is more frequent in areas with greater VW challenges and has thus been selectively favored during subsequent breeding processes.

Nevertheless, we aimed to gain further insight into the negative selection of *GhCBSX3A_R* during domestication, so we evaluated other traits in the 419 accessions. We found that accessions with the *GhCBSX3A_S* allele exhibited significantly larger BW compared to those carrying *GhCBSX3A_R*. However, there were no significant variations in three fiber-yield traits (lint percentage, seed index, and fiber weight per boll [FWPB]) or six fiber-quality traits (fiber length, fiber strength, micronaire, elongation, maturity, spinning consistency index) between the two haplotypes (Figure S3). This suggests that the selection for larger BW has driven the negative selection of *GhCBSX3A_R* during domestication.

To explore the presence of selective sweeps, we analyzed the genetic diversity of the *GhCBSX3A* locus and its surrounding regions in both cultivars and wild/landrace accessions. The nucleotide diversity (π) at the *GhCBSX3A* locus significantly declined in both cultivars and wild/landrace accessions, and decreasing from 0.55×10^{-3} in the wild/landrace accessions to 0.13×10^{-3} in cultivars group (Figure 6h). This reduction indicates that the locus has been subjected to artificial selection. Finally, we assessed genomic differentiation between wild/landrace accessions and early improved accession. Using an F_{ST} threshold of >0.343 (top 10%) to identify sweep regions, we found that the *GhCBSX3A* locus exhibited strong differentiation above this threshold (Figure 6h). These findings further support the hypothesis of artificial selection at the *GhCBSX3A* locus during the domestication process.

DISCUSSION

Verticillium wilt is considered as a major threat to cotton production, yet the genetic basis of quantitative variation for VW resistance in cotton remains poorly understood. This lack of understanding hampers targeted-genotyping-based selection in current resistance breeding strategies, making it challenging to achieve broad-spectrum disease resistance. To further investigate the mechanism underlying VW resistance in *G. hirsutum*, we previously conducted a GWAS on VW resistance using a large-scale upland cotton germplasm resource. We found a significant VW-associated locus on A10, which appears to be an introgressed fragment from *G. arboreum*, contributed to VW resistance in upland cotton (Zhang, Zhang, Ge, et al., 2023). Numerous studies have suggested that VW resistance in cotton is a complex, quantitative trait influenced by multiple quantitative trait loci and functional genes (Shaban et al., 2018). Consequently, we further

examined the function of the *AYDI3/AYDP2* locus, which showed a similar significant correlation to VW resistance as the A10 locus. Within the *AYDI3/AYDP2* locus, we found that the strong VW resistance correlation stemmed from a significant resistance enhancement of Hap. A. Interestingly, Hap. A was markedly distinct from other susceptible groups but showed high similarity to a cluster composed of wild/landrace accessions. Further analysis indicated that strong differentiation in *AYDI3/AYDP2* locus has long existed among the wild/landrace accessions. This differentiation led to the formation of Hap. A to Hap. D following long period of artificial selection.

Contrasting with marker-assisted breeding, biological breeding represents a new direction for major crops, with the identification of key genes underlying important traits being crucial for this new approach. In this study, we found that *GhCBSX3A*, which was induced post-*V. dahliae* infection, is the causal gene for the *AYDI3/AYDP2* locus. Silencing *GhCBSX3A* expression reduced SAR-RBOHs-mediated ROS accumulation during *V. dahliae* infection in cotton. Conversely, the overexpression of *GhCBSX3A* enhanced resistance to *V. dahliae* by contributing to both PTI- and SAR-ROS production, coupled with the induction of RBOHs expression. These findings underscore the importance of *GhCBSX3A* in facilitating the apoplastic oxidative burst during *V. dahliae* invasion in plants. Unlike *CBSX1* and *CBSX2* from *A. thaliana*, which directly regulate activation of TRXs as redox regulators in chloroplasts, and *AtCBSX3*'s contribution to ROS generation in mitochondrial complex 2, *GhCBSX3A* primarily localizes to the plasma membrane (Figure S4b), akin to the pathogen-resistant homolog in wheat (*TaCBSX3*) (Wang, Guo, et al., 2022). This makes our study identify a functional CBSX protein in pathogen resistance, mediated by regulation of the apoplastic oxidative burst. In plant cells, the apoplast, chloroplasts, mitochondria, and peroxisomes can produce ROS. Integrating previous studies with our findings, it appears that the CBSX protein family is involved in ROS production in three major organelles: the apoplast, the mitochondria, and the chloroplast. This makes CBSX proteins act as broad-spectrum redox modulators, influencing not only cell wall thickening and plant development but also pathogen resistance. Given that *TaCBSX3* interacts with *TaGSTU6* in the plasma membrane to jointly facilitate pathogen resistance, and considering the well-characterized role of GST proteins in regulating ROS accumulation in response to both biotic and abiotic stress (Le Martret et al., 2011; Pennington et al., 2016; Wang, Zhang, et al., 2022), it is plausible that cotton may possess GST proteins that collaborate with *GhCBSX3A* in defending against pathogens.

Meanwhile, we have observed considerable differences in the expression patterns of RBOHs between Arabidopsis and cotton. For example, *AtRBOHB*, whose

homologous gene was induced in cotton, is not triggered by *V. dahliae* in wild-type Arabidopsis. This suggests a disparity in the *V. dahliae*-mediated ROS burst between cotton and Arabidopsis.

In eukaryotes, RNA polymerase II (Pol II) is responsible for transcribing nuclear genes that encode mRNAs. A crucial aspect of this involves the TATA box-binding protein (TBP) recognizing the TATA-box, acting as the primary DNA anchor of this complicated macromolecular machine. Thus, the TATA-box is a key regulatory element, with sequence-specific interactions between TBP and TATA-box directly determining gene expression patterns. A previous study identified the deletion of the TATA-box from the *GhPRE1D* promoter as the causal agent for gene silencing in diploid species, mediating the variation in cotton fiber elongation (Zhao et al., 2018). Similarly, the allelic insertion of a TATA-box, -363 to -357 bp from the TSS of *IRT1*, enabled apple to adapt to selective pressure posed by Fe deficiency (Zhang et al., 2017). Another study found that the substitution from T to C at the third nucleotide bases significantly reduced the transcriptional activity of TATA-box (Patikoglou et al., 1999), akin to the variation from *GhCBSX3A_R* to *GhCBSX3A_S*. Our research demonstrates that sequence variations in the TATA-box contribute to significant expression differences in pathogen-resistant genes. Although both haplotypes exhibited expression differences pre- and post-inoculation with *V. dahliae*, both haplotypes up-regulated expression after *V. dahliae* invasion. This result indicated that substitution of the TATA-box altered the core-transcriptional machinery without affecting the pathogen-induced process. This suggests that other *cis*-elements (e.g., two predicted TCA-elements, involved in salicylic acid responsiveness) (Lescot et al., 2002) might facilitate these responses.

Our research revealed that the cultivars carrying *GhCBSX3A_R* are more resistant to VW than those carrying *GhCBSX3A_S*, due to an enhancement in gene expression. However, we observed no discernible variation in VW resistance between the two haplotypes in wild/landrace accessions. The incomplete functionality of *GhCBSX3A_R* in wild/landrace accessions requires further investigation. We hypothesize that the domestication process from wild/landrace accessions to elite lines has altered the signaling pathways downstream of *GhCBSX3A*. This could explain the differing contributions of *GhCBSX3A_R* to VW resistance before and after artificial selection.

Interestingly, the loss of the *GhCBSX3A_R* allele during the transition from wild/landrace accessions to improved upland cotton led to a decrease in VW resistance in the early improved lines. As for the reason which produces, we showed that during early upland cotton domestication, the high expression mediated by *GhCBSX3A_R* induced a reduction of BW, an agronomic trait likely not favored during domestication. Coupled together with an

absence of VW pressures, these factors likely contributed to the negative selection during domestication. Therefore, high expression of *GhCBSX3A* seems disadvantageous for cotton boll development in environments with low VW pressures, possibly due to a 'defense cost' where activated immunity negatively affects plant growth (He et al., 2022). Indeed, overexpression of *GhCBSX3A* in *A. thaliana* has been shown to positively regulate PTI and SAR, leading to a decrease in root length (Figure 5e). However, early human selection for *GhCBSX3A* appears to only focus on presentative BW, without contribution to fiber yield, as indicated by the lack of significant difference in FWPB. Furthermore, in regions like Xinjiang, the world's largest cotton production area, a smaller BW with constant FWPB could be more advantageous for maintaining stable total yields, which is urgently needed to improve crops (Yang et al., 2023). Therefore, accessions carrying the *GhCBSX3A_R* allele are expected to contribute to the development of novel cotton varieties.

In the breeding process, we established that increasing the proportion of *GhCBSX3A_R* correlates with continuous enhancement of VW resistance, particularly in regions facing greater VW challenges. This trend is likely due to the widespread epidemic of VW and corresponding significant losses in contemporary cotton production, as well as that modern breeding practices tend to be more comprehensive, focusing on both fiber yield and fiber quality being the primary breeding goals.

CONCLUSION

In conclusion, our study identified *GhCBSX3A*, encoding a CBS domain protein, as a causal gene underlying the A13 locus, which is significantly associated with VW resistance in *G. hirsutum*. Allelic variation in the TATA-box of the *GhCBSX3A* promoter promotes higher expression and a more robust SAR-RBOHs-mediated apoplastic oxidative burst, thereby enhancing VW resistance in Hap. A. We discovered that the elite *GhCBSX3A_R* allele, advantageous for VW resistance, underwent negative selection during the domestication process, leading to a reduction in VW resistance in early improved accessions. However, it was positively selected in subsequent breeding processes, resulting in a continual enhancement of VW resistance. Our results suggested the altered artificial selection of *GhCBSX3A_R* based on variant VW pressures. Our study highlights the role of *GhCBSX3A* in cotton VW disease and proposes a model where defense-associated genes are selected depending on the pathogen's pressure.

EXPERIMENTAL PROCEDURES

Plant materials and VW resistance phenotyping

Our GWAS on VW resistance phenotyping was consistent with our previous study (Zhang, Zhang, Ge, et al., 2023). All 419

accessions were cultivated in a disease nursery in Anyang, Henan, China, where they were exposed to *V. dahliae* strains Vd076, Vd080, and Vd991 in advance. The phenotyping evaluations followed the methodology described previously (Zhang et al., 2019), with assessments taking place when the susceptible control (JM11) displayed typical symptoms of Verticillium wilt and reached a DI of 51.05.

Regarding the investigation of the artificial selection process in VW resistance, we referred to previous studies for the relative DI of total *G. hirsutum* 458 accessions (421 cultivars and 37 landraces) in greenhouse (Zhang et al., 2021; Zhang, Zhang, Gao, et al., 2023). In brief, seedlings were grown for 2 weeks in a growth chamber under a 16 h photoperiod and temperatures of $28 \pm 2^\circ\text{C}$ (day) and $25 \pm 2^\circ\text{C}$ (night). The highly pathogenic strain *V. dahliae* isolate, LX2-1, was used for inoculation (10 ml conidia with $10^7/\text{ml}$). Symptom development was recorded at 20 days post-inoculation and graded from zero to four (Zhang et al., 2021).

Plasmid construction and transformation

For the luciferase reporters used in the transient expression assay, we amplified a 3000-bp fragment upstream of the ATG start codon of *GhCBSX3A* from Hap. A (B061) and Hap. B (L109). These fragments served as the full-length promoter, while truncated promoter sequences of *GhCBSX3A* were amplified from vectors containing the corresponding full-length promoters using different primer pairs (Table S3). These fragments were then inserted into *Sall* and *KpnI* digested pGreenII0800-LUC (Xie et al., 2017) to produce *CBSX3A_R_{pro}-1::LUC*, *CBSX3A_S_{pro}-1::LUC*, *CBSX3A_R_{pro}-2::LUC*, and *CBSX3A_S_{pro}-2::LUC*. To further analyze the function of *cis*-elements in the putative promoters, a 91-bp 35S minimal promoter was first inserted into the *Sall* and *Bam*HI digested pGreenII0800-LUC, producing the pGreenII0800-35Smini-LUC construct (Chen et al., 2019). Truncated promoter sequences of *GhCBSX3A* and three tandem copies of the TATA-box core sequence were then inserted into *Sall* and *KpnI* digested pGreenII0800-35Smini-LUC to produce a series of *GhCBSX3A_{pro}-mini::LUC* derivatives and *TATA-mini::LUC*.

For the VIGS experiments, we amplified 200–300 bp fragments from *GhCBSX3* coding sequences from B061. Subsequently, these fragments were inserted into *Xba*I and *Bam*HI digested pYL156. For the heterologous expression experiments, we amplified full-length coding sequences of *GhCBSX3A* from B061 and inserted them into *Xba*I and *Pac*I digested pCambia2300. We used *Agrobacterium tumefaciens* strain GV3101, harboring recombinant pCambia2300 vector under a control of 35S promoter, to generate the overexpressed transgenic Arabidopsis.

VIGS in upland cotton

For the VIGS assays, we utilized the *A. tumefaciens* strain GV3101, harboring pYL156 plasmids, and combined it with strains harboring pYL192 vectors (Zhang, Wu, Yu, et al., 2023). These were mixed in a 1:1 ratio and co-infiltrated into the cotyledons of 2-week-old cotton plants (B061). TRV::*CLA1* (*chloroplasts alterados 1* gene) was used as a positive control. One week later, the leaves from three individuals were harvested for RNA extraction, then we conducted qRT-PCR analyses to assess the expression levels of the target gene.

SNP-based phylogenetic tree

We analyzed SNPs from 419 *G. hirsutum* and our GWAS panel using GATK 3.8 software, following a previous report (Ma

et al., 2018). A total of 7062 SNPs were identified within the haplotype block (87.55–88.29 Mb) on *AYDI3/AYDP2* locus. SNPs were used to construct a phylogenetic tree using FastTree with default parameters (Price et al., 2009). To further exclude the introgression from *G. arboreum* and *G. barbadense*, we identified SNPs from *G. arboreum*, *G. barbadense*, and *G. hirsutum* landraces within the haplotype block to construct an expanded SNP-based phylogenetic tree.

RNA extraction and qRT-PCR

We extracted total RNA from cotton and *A. thaliana* seedlings using the RNAprep Pure Plant Kit (Tiangen, Beijing, China). Subsequently, cDNA was synthesized using the PrimeScript™ RT Reagent Kit with a gDNA Eraser (Takara, Tokyo, Japan). For the qRT-PCR analyses, we used SYBR® Premix Ex Taq™ (Takara) on an ABI 7900 Real-Time PCR System (Applied Biosystems, Bedford, MA, USA). All the qRT-PCR primers were designed using the Primer Premier 6.0 software and are listed in Table S3.

mRNA-seq analysis

We harvested the cotton roots at 24 hpi treated with Vd080 or water for ZZZ (resistance) plants. We used mRNA-seq data for screening the candidate genes within *AYDI3/AYDP2* locus. We obtained clean reads by removing all reads containing adapters and poly-N, which were low-quality reads from the raw read data. The filtered reads were then mapped to the *G. hirsutum* reference genome (CRI-TM-1, version 1.0) using Hisat2 software (Kim et al., 2015). Differential expression analysis was performed with the ‘EdgeR’ package in R (Wang, Hu, et al., 2023).

Chemical staining

For 3, 3'-diaminobenzidine (DAB) staining, we vacuum-infiltrated the leaves with a 1 mg ml^{-1} DAB solution for 30 min. Subsequently, the infiltrated leaves were kept in the dark for 16 h and then destained in 90% ethanol before imaging. Nitroblue tetrazolium staining was performed as previously described (Huang et al., 2019). The total amounts of H_2O_2 in root cells were determined by measuring the UV-Vis absorbance peak using tetramethylbenzidine solution incubated with GOx-NCs and glucose (Li, Zang, et al., 2021).

V. dahliae culture and plant inoculation

The *V. dahliae* strain, Vd080, was obtained from the Institute of Cotton Research of the Chinese Academy of Agricultural Sciences. We prepared *V. dahliae* as described previously (Zhang et al., 2019). Each cotton plant was inoculated with 10 ml of *V. dahliae* suspension ($\sim 1 \times 10^7$ conidia ml^{-1}) using the root dip method.

Arabidopsis thaliana sterile seedlings were grown on plate with Murashige and Skoog medium for 2 weeks, then they were transferred to soil for an additional 3 weeks growing. We inoculated each plant with 10 ml of *V. dahliae* suspension ($\sim 1 \times 10^7$ conidia ml^{-1}) by injection into the surrounding soil. We investigated Verticillium wilt phenotypes 2 days post-inoculation. The DI for *A. thaliana* plants was calculated as previously described (Veronese et al., 2003).

V. dahliae recovery assays

To further assess cotton resistance to Verticillium wilt, we isolated *V. dahliae* from the first stem nodes of the TRV::00 and TRV::

GhCBSX3A. Stem segments (4.5 cm) were first surface-disinfested for 5 min in NaClO (active chlorine >5%) and then cut into five parts. The stem fragments were placed on potato dextrose agar plates and incubated at 25°C for 7 days. For recovery assays with *A. thaliana*, the main stems were surface-disinfested with 95% ethyl alcohol and then cut into six sections.

Luciferase assays

We inoculated *Nicotiana benthamiana* leaves with *A. tumefaciens* carrying LUC reporter vectors. After inoculation, the plants were grown in the dark for 2 days. The fluorescence intensity was captured using a Tanon 5200 Multi Chemiluminescent Imaging System. We also measured the luciferase activity using the Dual-Luciferase Reporter Assay System (Promega, Madison, WI, USA) following the manufacturer's protocol. The relative firefly luciferase activity was calculated as the ratio of firefly luciferase to Renilla luciferase activity (LUC/REN) (Xie et al., 2017; Zhu et al., 2023).

ROS burst assays

We performed the ROS burst assay as described previously with slight modifications (Li, Zhao, et al., 2021; Liang et al., 2013). Briefly, we excised the leaf disks ($r=0.2$ cm) for *A. thaliana* leaves and incubated three disks per well in a 48-well plate with water overnight. After incubation, the water was removed from each well and replaced with 200 μ l chemiluminescent luminol buffer containing 200 mM luminol (Sigma, St. Louis, MO, USA), 20 g ml⁻¹ horseradish peroxidase (Sigma) and elicitors (MeSA and Flg22). Flg22 (Genescript, Nanjing, China) and MeSA (Sigma) were stored in water and methanol respectively. We then dissolved these into the water for 2 mM Flg22 and 400 mM MeSA, respectively. Luminescence was subsequently recorded by the BioTek-Synergy-HT outfitted with the LUM module.

AUTHOR CONTRIBUTIONS

ZY and FL conceived and designed the research. ZY managed the project. ZY, YiZ, YY, YaZ, CG, MM, HX, and QH prepared the samples, performed phenotyping, and contributed to data analysis. YiZ and YaZ designed and performed the molecular experiments. YiZ prepared the figures and tables. YiZ and ZY wrote and revised the manuscript.

ACKNOWLEDGEMENTS

This work was supported by funding from the Key Research and Development Project of Henan Province (231111110400), the National Key Research and Development Program (2021YFF1000102-1), Natural Science Foundation of Henan (No. 232300421010), Central Public-interest Scientific Institution Basal Research Fund (No. Y2023XK16), Innovation Program of the Chinese Academy of Agricultural Sciences (CAASASTIP-IVFCAAS), the Fundamental Research Funds of State Key Laboratory of Cotton Biology (CB2021E03), and Innovation Program of Chinese Academy of Agricultural Sciences (CAAS-CSIAF-202302). We would like to thank Prof. Xiaoyang Ge and Prof. Hang Zhao for their constructive comments. We thank Dr. Savannah Grace at the University of Florida for her assistance with the English language and grammatical editing of the manuscript.

CONFLICT OF INTEREST

The authors declare no conflicts of interest.

DATA AVAILABILITY STATEMENT

The authors confirm that all relevant data can be found within the manuscript and its supporting materials.

SUPPORTING INFORMATION

Additional Supporting Information may be found in the online version of this article.

Figure S1. Essential information of GhCBSX3A amino acid sequence.

Figure S2. The positive control of VIGS (TRV::CLA1).

Figure S3. Comparison of agronomic trait of accessions carrying either the *GhCBSX3A_R* or *GhCBSX3A_S* alleles.

Figure S4. Seed germination of 35S::GhCBSX3A lines and subcellular localization assays of GhCBSX3A.

Table S1. Swissprot annotation of candidate genes in AYDI3/AYDP2 locus.

Table S2. GhCBSX3A_R haplotype, geographical distribution and breeding years of *G. hirsutum* accessions.

Table S3. Primer sequences used in this study.

REFERENCES

- Ali, F., Li, Y., Li, F. & Wang, Z. (2021) Genome-wide characterization and expression analysis of cystathionine β -synthase genes in plant development and abiotic stresses of cotton (*Gossypium* spp.). *International Journal of Biological Macromolecules*, **193**, 823–837.
- Chang, Y., Li, B., Shi, Q., Geng, R., Geng, S., Liu, J. et al. (2020) Comprehensive analysis of respiratory burst oxidase homologs (Rboh) gene family and function of *GbRboh5/18* on Verticillium wilt resistance in *Gossypium barbadense*. *Frontiers in Genetics*, **11**, 788.
- Chen, Q., Xu, X., Xu, D., Zhang, H., Zhang, C. & Li, G. (2019) WRKY18 and WRKY53 coordinate with HISTONE ACETYLTRANSFERASE1 to regulate rapid responses to sugar. *Plant Physiology*, **180**, 2212–2226.
- Gruner, K., Zeier, T., Aretz, C. & Zeier, J. (2018) A critical role for Arabidopsis MILDEW RESISTANCE LOCUS O2 in systemic acquired resistance. *The Plant Journal*, **94**, 1064–1082.
- He, S., Sun, G., Geng, X., Gong, W., Dai, P., Jia, Y. et al. (2021) The genomic basis of geographic differentiation and fiber improvement in cultivated cotton. *Nature Genetics*, **53**, 916–924.
- He, Z., Webster, S. & He, S. (2022) Growth–defense trade-offs in plants. *Current Biology*, **32**, R634–R639.
- Heller, J. & Tudzynski, P. (2011) Reactive oxygen species in phytopathogenic fungi: signaling, development, and disease. *Annual Review of Phytopathology*, **49**, 369–390.
- Huang, L., Yu, L.J., Zhang, X., Fan, B., Wang, F.Z., Dai, Y.S. et al. (2019) Autophagy regulates glucose-mediated root meristem activity by modulating ROS production in Arabidopsis. *Autophagy*, **15**, 407–422.
- Kahlon, P.S., Seta, S.M., Zander, G., Scheikl, D., Hückelhoven, R., Joosten, M. et al. (2020) Population studies of the wild tomato species *Solanum chilense* reveal geographically structured major gene-mediated pathogen resistance. *Proceedings of the Biological Sciences*, **287**, 20202723.
- Kim, D., Langmead, B. & Salzberg, S.L. (2015) HISAT: a fast spliced aligner with low memory requirements. *Nature Methods*, **12**, 357–360.
- Kushwaha, H.R., Singh, A.K., Sopory, S.K., Singla-Pareek, S.L. & Pareek, A. (2009) Genome wide expression analysis of CBS domain containing proteins in *Arabidopsis thaliana* (L.) Heynh and *Oryza sativa* L. reveals their developmental and stress regulation. *BMC Genomics*, **10**, 200.
- Lai, M., Cheng, Z., Xiao, L., Klosterman, S. & Wang, Y. (2022) The bZip transcription factor VdMRTF1 is a negative regulator of melanin biosynthesis and virulence in *Verticillium dahliae*. *Microbiology Spectrum*, **10**, e0258121.
- Le Martret, B., Poage, M., Shiel, K., Nugent, G.D. & Dix, P.J. (2011) Tobacco chloroplast transformants expressing genes encoding dehydroascorbate reductase, glutathione reductase, and glutathione-S-transferase, exhibit altered anti-oxidant metabolism and improved abiotic stress tolerance. *Plant Biotechnology Journal*, **9**, 661–673.

- Lescot, M., Déhais, P., Thijs, G., Marchal, K., Moreau, Y., Van de Peer, Y. *et al.* (2002) PlantCARE, a database of plant cis-acting regulatory elements and a portal to tools for in silico analysis of promoter sequences. *Nucleic Acids Research*, **30**, 325–327.
- Li, F., Zang, M., Hou, J., Luo, Q., Yu, S., Sun, H. *et al.* (2021) Cascade catalytic nanoplatfrom constructed by laterally-functionalized pillar[5]arenes for antibacterial chemodynamic therapy. *Journal of Materials Chemistry B*, **9**, 5069–5075.
- Li, P., Zhao, L., Qi, F., Htwe, N., Li, Q., Zhang, D. *et al.* (2021) The receptor-like cytoplasmic kinase RIPK regulates broad-spectrum ROS signaling in multiple layers of plant immune system. *Molecular Plant*, **14**, 1652–1667.
- Li, T., Ma, X., Li, N., Lei, Z. & Zheng, L. (2017) Genome-wide association study discovered candidate genes of *Verticillium* wilt resistance in upland cotton (*Gossypium hirsutum* L.). *Plant Biotechnology Journal*, **15**, 1520–1532.
- Li, Y.B., Han, L.B., Wang, H.Y., Zhang, J., Sun, S.T., Feng, D.Q. *et al.* (2016) The thioredoxin GbNFX1 plays a crucial role in homeostasis of apoplastic reactive oxygen species in response to *Verticillium dahliae* infection in cotton. *Plant Physiology*, **170**, 2392–2406.
- Liang, Y., Cao, Y., Tanaka, K., Thibivilliers, S., Wan, J., Choi, J. *et al.* (2013) Nonlegumes respond to rhizobial Nod factors by suppressing the innate immune response. *Science*, **341**, 1384–1387.
- Liu, Y. & Zhang, H. (2021) Reactive oxygen species and nitric oxide as mediators in plant hypersensitive response and stomatal closure. *Plant Signaling & Behavior*, **16**, 1985860.
- Lunn, D., Smith, G.A., Wallis, J.G. & Browse, J. (2022) Overexpression mutants reveal a role for a chloroplast MPD protein in regulation of reactive oxygen species during chilling in Arabidopsis. *Journal of Experimental Botany*, **73**, 2666–2681.
- Ma, Z., He, S., Wang, X., Sun, J., Zhang, Y., Zhang, G. *et al.* (2018) Resequencing a core collection of upland cotton identifies genomic variation and loci influencing fiber quality and yield. *Nature Genetics*, **50**, 803–813.
- Morales, J., Kadota, Y., Zipfel, C., Molina, A. & Torres, M.A. (2016) The Arabidopsis NADPH oxidases *RbohD* and *RbohF* display differential expression patterns and contributions during plant immunity. *Journal of Experimental Botany*, **67**, 1663–1676.
- Mou, S., Shi, L., Lin, W., Liu, Y., Shen, L., Guan, D. *et al.* (2015) Overexpression of rice CBS domain containing protein, *OscBSX3*, confers rice resistance to *Magnaporthe oryzae* inoculation. *International Journal of Molecular Sciences*, **16**, 15903–15917.
- Patikoglou, G.A., Kim, J.L., Sun, L., Yang, S.H., Kodadek, T. & Burley, S.K. (1999) TATA element recognition by the TATA box-binding protein has been conserved throughout evolution. *Genes & Development*, **13**, 3217–3230.
- Pennington, H.G., Gheorghe, D.M., Damerum, A., Pliego, C., Spanu, P.D., Cramer, R. *et al.* (2016) Interactions between the powdery mildew effector BEC1054 and barley proteins identify candidate host targets. *Journal of Proteome Research*, **15**, 826–839.
- Price, M., Dehal, P. & Arkin, A. (2009) FastTree: computing large minimum evolution trees with profiles instead of a distance matrix. *Molecular Biology and Evolution*, **26**, 1641–1650.
- Qi, J., Song, C., Wang, B., Zhou, J., Kangasjärvi, J., Zhu, J. *et al.* (2018) Reactive oxygen species signaling and stomatal movement in plant responses to drought stress and pathogen attack. *Journal of Integrative Plant Biology*, **60**, 805–826.
- Shaban, M., Miao, Y., Ullah, A., Khan, A.Q., Menghwar, H., Khan, A.H. *et al.* (2018) Physiological and molecular mechanism of defense in cotton against *Verticillium dahliae*. *Plant Physiology and Biochemistry*, **125**, 193–204.
- Shin, J.S., So, W.M., Kim, S.Y., Noh, M., Hyoung, S., Yoo, K.S. *et al.* (2020) CBSX3-Trxo-2 regulates ROS generation of mitochondrial complex II (succinate dehydrogenase) in Arabidopsis. *Plant Science*, **294**, 110458.
- Tan, W. (1994) Causes and control strategy of verticillium wilt outbreak in northern cotton region. *China Cotton*, **21**, 2–4.
- Veronese, P., Narasimhan, M.L., Stevenson, R.A., Zhu, J.K., Weller, S.C., Subbarao, K.V. *et al.* (2003) Identification of a locus controlling *Verticillium* disease symptom response in *Arabidopsis thaliana*. *The Plant Journal*, **35**, 574–587.
- Vlot, A.C., Sales, J.H., Lenk, M., Bauer, K., Brambilla, A., Sommer, A. *et al.* (2021) Systemic propagation of immunity in plants. *The New Phytologist*, **229**, 1234–1250.
- Wang, D., Hu, X., Ye, H., Wang, Y., Yang, Q., Liang, X. *et al.* (2023) Cell-specific clock-controlled gene expression program regulates rhythmic fiber cell growth in cotton. *Genome Biology*, **24**, 49.
- Wang, G., Wang, X., Song, J., Wang, H., Ruan, C., Zhang, W. *et al.* (2023) Cotton peroxisome-localized lysophospholipase counteracts the toxic effects of *Verticillium dahliae* NLP1 and confers wilt resistance. *The Plant Journal*, **115**, 452–469.
- Wang, H. (2015) Review on damage of cotton fusarium and *Verticillium* wilt in China and breeding for disease resistance. *Chinese Agricultural Science Bulletin*, **31**, 124–130.
- Wang, Q., Guo, J., Jin, P., Guo, M., Guo, J., Cheng, P. *et al.* (2022) Glutathione S-transferase interactions enhance wheat resistance to powdery mildew but not wheat stripe rust. *Plant Physiology*, **190**, 1418–1439.
- Wang, S., Wu, X.M., Liu, C.H., Shang, J.Y., Gao, F. & Guo, H.S. (2020) *Verticillium dahliae* chromatin remodeling facilitates the DNA damage repair in response to plant ROS stress. *PLoS Pathogens*, **16**, e1008481.
- Wang, T., Zhang, D., Chen, L., Wang, J. & Zhang, W.H. (2022) Genome-wide analysis of the glutathione S-transferase family in wild *Medicago ruthenica* and drought-tolerant breeding application of *MruGSTU39* gene in cultivated alfalfa. *Theoretical and Applied Genetics*, **135**, 853–864.
- Wu, B., Yun, P., Zhou, H., Xia, D., Gu, Y., Li, P. *et al.* (2022) Natural variation in *WHITE-CORE RATE 1* regulates redox homeostasis in rice endosperm to affect grain quality. *Plant Cell*, **34**, 1912–1932.
- Xie, Y., Liu, Y., Wang, H., Ma, X., Wang, B., Wu, G. *et al.* (2017) Phytochrome-interacting factors directly suppress MIR156 expression to enhance shade-avoidance syndrome in Arabidopsis. *Nature Communications*, **8**, 348.
- Yang, Z., Gao, C., Zhang, Y., Yan, Q., Hu, W., Yang, L. *et al.* (2023) Recent progression and future perspectives in cotton genomic breeding. *Journal of Integrative Plant Biology*, **65**, 548–569.
- Zhang, L., Wu, Y., Yu, Y., Zhang, Y., Wei, F., Zhu, Q.H. *et al.* (2023) Acetylation of GhCaM7 enhances cotton resistance to *Verticillium dahliae*. *The Plant Journal*, **114**, 1405–1424.
- Zhang, M., Lv, Y., Wang, Y., Rose, J.K., Shen, F., Han, Z. *et al.* (2017) TATA box insertion provides a selection mechanism underpinning adaptations to Fe deficiency. *Plant Physiology*, **173**, 715–727.
- Zhang, Y., Chen, B., Sun, Z., Liu, Z., Cui, Y., Ke, H. *et al.* (2021) A large-scale genomic association analysis identifies a fragment in Dt11 chromosome conferring cotton *Verticillium* wilt resistance. *Plant Biotechnology Journal*, **19**, 2126–2138.
- Zhang, Y., Jin, Y., Gong, Q., Li, Z., Zhao, L., Han, X. *et al.* (2019) Mechanism analysis of resistance to *Verticillium dahliae* in upland cotton conferred by overexpression of *RPL18A-6* (ribosomal protein L18A-6). *Industrial Crops and Products*, **141**, 111742.
- Zhang, Y., Zhang, Y., Gao, C., Zhang, Z., Yuan, Y., Zeng, X. *et al.* (2023) Uncovering genomic and transcriptional variations facilitates utilization of wild resources in cotton disease resistance improvement. *Theoretical and Applied Genetics*, **136**, 204.
- Zhang, Y., Zhang, Y., Ge, X., Yuan, Y., Jin, Y., Wang, Y. *et al.* (2023) Genome-wide association analysis reveals a novel pathway mediated by a dual-TIR domain protein for pathogen resistance in cotton. *Genome Biology*, **24**, 111.
- Zhang, Z., Zhao, J., Ding, L., Zou, L., Li, Y., Chen, G. *et al.* (2016) Constitutive expression of a novel antimicrobial protein, Hcm1, confers resistance to both *Verticillium* and *Fusarium* wilts in cotton. *Scientific Reports*, **6**, 20773.
- Zhao, B., Cao, J.F., Hu, G.J., Chen, Z.W., Wang, L.Y., Shangguan, X.X. *et al.* (2018) Core cis-element variation confers subgenome-biased expression of a transcription factor that functions in cotton fiber elongation. *The New Phytologist*, **218**, 1061–1075.
- Zhao, Y., Chen, W., Cui, Y., Sang, X., Lu, J., Jing, H. *et al.* (2021) Detection of candidate genes and development of *KASP* markers for *Verticillium* wilt resistance by combining genome-wide association study, QTL-seq and transcriptome sequencing in cotton. *Theoretical and Applied Genetics*, **134**, 1063–1081.
- Zhu, F., Zhu, P.X., Xu, F., Che, Y.P., Ma, Y.M. & Ji, Z.L. (2020) Alphanomocharin enhances *Nicotiana benthamiana* resistance to tobacco mosaic virus infection through modulation of reactive oxygen species. *Molecular Plant Pathology*, **21**, 1212–1226.
- Zhu, W., Miao, X., Qian, J., Chen, S., Jin, Q., Li, M. *et al.* (2023) A translome-transcriptome multi-omics gene regulatory network reveals the complicated functional landscape of maize. *Genome Biology*, **24**, 60.